

# Proteomic Basis of Stress Responses in the Gills of the Pacific Oyster *Crassostrea gigas*

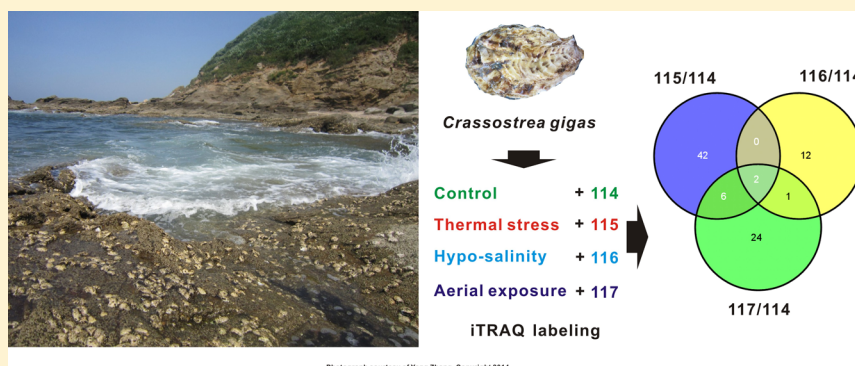
Yang Zhang,<sup>||,†</sup> Jin Sun,<sup>||,‡</sup> Huawei Mu,<sup>‡</sup> Jun Li,<sup>†</sup> Yuehuan Zhang,<sup>†</sup> Fengjiao Xu,<sup>†</sup> Zhiming Xiang,<sup>†</sup> Pei-Yuan Qian,<sup>§</sup> Jian-Wen Qiu,<sup>\*,‡</sup> and Ziniu Yu<sup>\*,†</sup>

<sup>†</sup>Key Laboratory of Tropical Marine Bio-resources and Ecology, South China Sea Institute of Oceanology, Chinese Academy of Sciences, 164 West Xingang Road, Guangzhou 510301, China

<sup>‡</sup>Department of Biology, Hong Kong Baptist University, Kowloon Tong, Hong Kong, China

<sup>§</sup>Division of Life Science, The Hong Kong University of Science and Technology, Hong Kong, China

## S Supporting Information



**ABSTRACT:** The Pacific oyster *Crassostrea gigas* is one of the dominant sessile inhabitants of the estuarine intertidal zone, which is a physically harsh environment due to the presence of a number of stressors. Oysters have adapted to highly dynamic and stressful environments, but the molecular mechanisms underlying such stress adaptation are largely unknown. In the present study, we examined the proteomic responses in the gills of *C. gigas* exposed to three stressors (high temperature, low salinity, and aerial exposure) they often encounter in the field. We quantitatively compared the gill proteome profiles using iTRAQ-coupled 2-D LC–MS/MS. There were 3165 identified proteins among which 2379 proteins could be quantified. Heat shock, hyposalinity, and aerial exposure resulted in 50, 15, and 33 differentially expressed gill proteins, respectively. Venn diagram analysis revealed substantial different responses to the three stressors. Only xanthine dehydrogenase/oxidase showed a similar expression pattern across the three stress treatments, suggesting that reduction of ROS accumulation may be a conserved response to these stressors. Heat shock caused significant overexpression of molecular chaperones and production of *S*-adenosyl-L-methionine, indicating their crucial protective roles against protein denature. In addition, heat shock also activated immune responses, Ca<sup>2+</sup> binding protein expression. By contrast, hyposalinity and aerial exposure resulted in the up-regulation of 3-demethylubiquinone-9 3-methyltransferase, indicating that increase in ubiquinone synthesis may contribute to withstanding both the osmotic and desiccation stress. Strikingly, the majority of desiccation-responsive proteins, including those involved in metabolism, ion transportation, immune responses, DNA duplication, and protein synthesis, were down-regulated, indicating conservation of energy as an important strategy to cope with desiccation stress. There was a high consistency between the expression levels determined by iTRAQ and Western blotting, highlighting the high reproducibility of our proteomic approach and its great value in revealing molecular mechanisms of stress responses.

**KEYWORDS:** oyster, gills, iTRAQ, *Crassostrea*, temperature, salinity, aerial exposure

## INTRODUCTION

The intertidal zone in estuaries is one of the most physically harsh and dynamic environments in the ocean, with widely fluctuated tidal levels and daily changes in temperature and salinity. Organisms living in the estuarine intertidal zone can thus be exposed to the air, low salinity, and high temperature (>40 °C) during the low tide. Consequently, such highly variable environmental conditions have shaped the adaptation

of intertidal estuarine communities. During the last several decades, the growing human activities as well as global climate change have imposed profound challenges on marine ecosystems. For example, the increasing atmospheric carbon

**Special Issue:** Environmental Impact on Health

**Received:** September 6, 2014

**Published:** November 12, 2014

dioxide concentration due to the burning of fossil fuels has caused acidification as well as warming of the ocean.<sup>1</sup> Global warming can intensify salinity variability of surface seawater, especially in inshore areas through increasing precipitation, and freshwater runoff.<sup>2</sup> Therefore, to survive, estuarine intertidal organisms must adapt to such harsh environments behaviorally and physiologically. For instance, tolerance to high temperature is often associated with the synthesis of molecular chaperones to stabilize denatured proteins and reducing metabolic demand,<sup>3</sup> while tolerance to hyposalinity often involves changes in intracellular free amino acid concentration to rapidly regulate cellular volume and osmolarity in intertidal marine mollusks.<sup>4–6</sup>

Among the intertidal inhabitants, the Pacific oyster *Crassostrea gigas* is a dominant sessile species in many estuarine intertidal zones throughout the temperate Pacific and Atlantic Oceans.<sup>7</sup> Unlike many other intertidal organisms, oysters are permanently attached to rock surfaces after settlement; therefore, they cannot escape from any abiotic or biotic stress affecting the intertidal zone. As a result, oysters have evolved to acquire powerful defense mechanisms to withstand the highly dynamic and stressful environments, which have made them an excellent model for studying stress adaptation.<sup>8</sup> Previous studies focusing on one to few genes have identified some important molecular mechanisms and key processes during stress adaptation or acclimatization in oyster gills and mantle. Specifically, a series of cell stress marker genes coding chaperone proteins (heat shock proteins (HSPs)), oxidative stress responsive proteins (Cu–Zn superoxide dismutase, metallothionein (MT), glutathione S-transferase), a transcriptional factor (hypoxia-inducible factor  $\alpha$ ), and osmoregulatory genes (amino acid transporter and taurine transporter) have been identified in oysters.<sup>3,9–13</sup> More recently, studies on the transcriptomic responses to stress based on systems biology tools, such as RNA-seq or microarray, have yielded important insights into the stress adaptation, leading to the discovery of over five thousand stress-responsive genes or gene sets in marine mollusks including oysters.<sup>8,14–18</sup> Up-regulation of HSPs and inhibition of apoptosis protein family (IAPs) is considered as the central mechanisms of oyster's amazing endurance to the stressful conditions in intertidal zone.<sup>8</sup> Moreover, some genes involved in signaling transduction, like G-protein-coupled receptors, Ras GTPase and PI3K/AKT/mTOR pathway, also played important roles in orchestrating the stress responses in oysters.<sup>8,19</sup>

However, transcriptional profiling may only partially contribute to the understanding of stress adaptation because not all transcripts can be translated and mRNA abundances may not correspond to protein expression level due to pre-, co-, and post-translational modification, and proteins, not mRNA, are the effectors of biological functions.<sup>20,21</sup> In addition, critical regulatory signaling events downstream of transcription will not be detected by transcript analysis.<sup>22</sup> Proteomics, the large-scale study of protein structures and functions, has the potential to fill this gap and enhance our understanding of the molecular mechanisms of stress responses in oysters and other intertidal animals.<sup>23</sup> A number of studies have characterized the proteomic responses to several stressors in oysters, including heavy metal exposure, elevated  $p\text{CO}_2$ , and pathogen infection.<sup>24–27</sup> However, to our knowledge, no proteomic studies have been conducted to understand the responses of oysters to temperature and salinity stressors. Of the previous studies on stress responses in oysters, most involved the use of the 2-D gel electrophoresis-based method, which suffers from

the shortcomings of low throughput and low reproducibility.<sup>28</sup> In the present study, we examined the proteomic responses of *C. gigas* to thermal stress (heat shock), hyposalinity, and aerial exposure in the gills because they are more exposed than many other organs to the environment and are known to be responsive to environmental challenges at the transcript level.<sup>14,15</sup> We adopted the isobaric tags for relative and absolute quantitation (iTRAQ) coupled to 2-D LC–MS/MS approach,<sup>29</sup> which is known to be a benchmarking technique in protein expression analysis with high throughput and high reproducibility,<sup>30,31</sup> to identify the proteins and determine the treatment effects. Moreover, we validated the expression results of a set of proteins determined by mass spectrometry (MS) using Western blotting. Here our study aimed to address the following questions: (1) Which proteins or functional groups of proteins alter their expressions significantly in response to the three stressors previously mentioned? (2) Are these responses specific or common to the three different stressors?

## ■ MATERIALS AND METHODS

### Oysters, Exposure Conditions, and Sample Collection

Two year old *C. gigas* (shell height 90–120 mm) were obtained from Qingdao, Shandong Province, China (120.33°E, 36.07°N), and maintained in the experiment station of South China Sea Institute of Oceanology (SCSIO), Chinese Academy of Sciences in Zhanjiang, Guangdong Province in February 2013. Oysters were acclimated in an aquarium tank (30 M<sup>3</sup>) supplied with sand-filtered seawater at ambient temperature ( $18 \pm 1$  °C) and salinity (30‰). Oysters were fed with the microalgae *Isochrysis galbana* (10<sup>5</sup> cell/mL) and *Chaetoceros calcitrans* (2 × 10<sup>5</sup> cell/mL) every day. The oysters were allowed to acclimate for 1 month. The experiment included a control and three treatments (heat shock: 38 °C for 1 h; hyposalinity: 8‰ for 24 h; aerial exposure: air at ambient temperature for 24 h), each with three replicates of four individuals. These exposure conditions were determined based on previous studies, which showed that experimental treatments are stressful to this species.<sup>15,16</sup> The 24 h exposure period for the hyposalinity and aerial exposure treatments roughly equals the tidal cycle (24 h and 52.7 min) in the oyster's native habitat. The oysters were kept in 50 L experimental tanks with sand-filtered and UV-sterilized seawater (30‰, except in the hyposalinity treatment). In the control, the seawater was maintained at ambient temperature ( $18 \pm 1$  °C). In the thermal stress treatment, the oysters were exposed to high temperature (38 °C) seawater for 1 h, followed by a 24 h recovery at ambient temperature ( $18 \pm 1$  °C).<sup>15,32</sup> In the hyposalinity treatment, the oysters were exposed to hyposalinity (8‰) for 24 h. The hyposaline seawater was prepared by dilution with filtered tap water, and the salinity was measured using a conductivity Meter (ATAGO, ES-421, Japan). In the aerial exposure treatment, the oysters were exposed to air in empty aquaria at ambient temperature for 24 h.

At the end of exposure, the oysters were dissected, and the gill tissues were used for proteomic analysis. In each oyster, sampling was conducted by excising ~100 mg gill tissue from each individual, and samples from four individuals were pooled to form one biological replicate. In total, 48 oysters representing three biological replicates of four experiment treatments (four treatments × three biological replicates × four

oysters per biological replicates) were used for the following protein analysis.

### Protein Extraction and iTRAQ Labeling

Gill samples dissolved in 8 M urea were homogenized and sonicated to break the cells and release the proteins. The samples were then centrifuged at 15 000g for 15 min at 4 °C. The supernatant was collected and transferred into a new tube. A 2D-cleanup Kit (Bio-Rad, Hercules, CA) was used to purify the samples, and the proteins were redissolved in 8 M urea. Each sample was quantified using a RC-DC Protein Assay Kit (Bio-Rad, Hercules, CA) following the manufacturer's protocol, and 200 µg protein from each replicate was used for iTRAQ labeling.<sup>33</sup> Proteins were reduced with 5 mM triscarboxyethyl phosphine hydrochloride at 60 °C for 1 h and alkylated with methylethanesulfonate (10 mM) for 20 min at room temperature. Triethylammonium bicarbonate (50 mM) was used to dilute the samples eight-fold, and the protein samples were digested for 16 h at 37 °C using sequencing-grade trypsin (Promega, Madison, WI) with a 1:50 (w:w) trypsin to protein ratio. After digestion, peptides from the control, heat shock, hyposalinity, and aerial exposure treatments were labeled with the isobaric tags 114, 115, 116, and 117, respectively. Samples were then pooled and dried in an Eppendorf vacuum concentrator.

### SCX Fractionation and LC-MS/MS Analysis

The dried samples were reconstituted using Solution A [20% acetonitrile (ACN) and 10 mM KH<sub>2</sub>PO<sub>4</sub>, pH 3.0]. SCX fractionation<sup>34</sup> was conducted by a Poly SULFOETHYL column (200 × 4.6 mm, 5 µm particle size, 200 Å pore size) (PolyLC, Columbia, MD) using a Waters 2695 HPLC. The fractionation was conducted for 50 min, with a flow rate of 1 mL/min. The fractionation involved the use of 100% Solution A for 5 min, then 0 to 30% Solution B (20% ACN, 10 mM KH<sub>2</sub>PO<sub>4</sub>, and 0.5 M KCl, pH 3.0) with a linear changing gradient for 28 min, 30 to 100% Solution B with a linear changing gradient for 5 min, 100% Solution B for 5 min, and 100% Solution A for 7 min. Fourteen fractions were collected, dried under vacuum, and desalted with Sep-Pak C18 cartridges (Waters, Milford, MA).

Samples were reconstituted with Solution A (0.1% formic acid in water) and analyzed with a LTQ-Orbitrap Elite (Thermo Fisher, Bremen, Germany) coupled to an Easy-nLC (Thermo Fisher, Bremen, Germany). Peptides were separated by a C18 capillary column (50 µm × 15 cm, packed with Acclaim PepMap RSLC C18, 2 µm, 100 Å, nanoViper, Thermo Scientific). A 90 min gradient was used, with 5 min in 100% Solution A, 55 min in 0–30% Solution B (0.1% formic acid in ACN), 10 min in 30–98% Solution B, 10 min in 98% Solution B, and finally 10 min in Solution A. A full MS scan (350–1600 *m/z* range) was acquired at a resolution of 60 000 in the positive charge mode. The five most abundant precursors with +2, +3, or +4 charges and over a minimum signal threshold of 500.0 were selected for fragmentation using a collision-induced dissociation (CID)/high-energy collision-induced dissociation (HCD) dual-scan approach. The peptide identification was resolved by CID spectra. At the same time, iTRAQ quantification was acquired in HCD in C-trap. The isolation width was set as 2.0 (*m/z*) for both HCD and CID with activated dynamic exclusion to remove the duplicate precursors. The settings for the CID scan were 35% for the normalized collision energy, 0.25 for the activation Q, and 10 ms for the activation time. The settings for the HCD fragmentation were

full-scan with FTMS at a resolution of 15 000 in a centroid mode, 45% normalized collision energy, and 10 ms activation time.

### Bioinformatics Analysis

Raw MS data were converted into .mgf files using Proteome Discoverer v 1.3 (Thermo Scientific). Unpaired scans (i.e., either CID or HCD profile without detecting the same precursor) were deleted. Both CID and HCD scans were applied for the same precursor. However, because of the limited quantity of a small percentage of precursors (<0.1%), either CID or HCD data were missing. For precursors with both CID and HCD data, the iTRAQ reporter mass (114.0–117.5 Da) from the HCD scans was extracted and used to replace the respective CID mass range using a python script. Data generated by HCD and the modified CID scans were then separately searched against *C. gigas* database based on DNA sequences submitted to NCBI,<sup>8</sup> including both the “target” sequences of 26 086 proteins and “decoy” sequences using Mascot version 2.3.2 (Matrix Sciences, London, U.K.). Parameters for CID scans were ±5 ppm for precursor, ±0.6 Da for fragments, up to two missed cleaved peptides, fixed modification of methylthio (cysteine), variable modification of deamidated glutamine, asparagine and oxidation of methionine, and the quantitation method of iTRAQ 4 plex. Searching criteria of HCD were similar to those of CID with the exception of 20 mmu of fragment tolerance. Ion scores of <28 which corresponded to 95% confidence level were discarded, and results were exported as .csv files.

False discovery rate threshold was set as 1%<sup>33</sup> for both CID and HCD database search. Unlabeled peptides and those matched to decoy database were deleted. For each protein, quantification was performed based on the summed intensity of peptides detected in both CID and HCD database search. Proteins with at least two peptides from any of the three replicates were kept. Median normalization was applied to each replicate.<sup>31</sup> The threshold for differentially expressed proteins (DEPs) was determined based on the 95% confidence level among the three biological replicates.<sup>33</sup> In other words, proteins that had a fold-change ratio >1.28 or <0.83 were considered as differentially expressed between control and treatment groups. Blast2GO was applied to classify the proteins into functional categories. GOEAST enrichment analysis was performed to determine the enriched protein categories, with all of the identified proteins being used as the background list.<sup>35</sup> In brief, all of the identified proteins annotated by Blast2GO and DEPs were submitted as “background list” and “gene list”, respectively. Enrichment analysis was performed by the hypergeometric test, and the significance level was corrected by the Yekutieli multitest FDR adjustment method.<sup>35</sup> Protein functional domains were deduced by searching against Pfam, which is a large collection of protein families.<sup>36</sup>

### Western Blotting

The extracted gill protein samples were homogenized and suspended in a cold lysis buffer containing 250 mM Tris/HCl (pH 8.0), 1% NP-40, and 150 mM NaCl. After centrifugation at 14 000g for 10 min at 4 °C, protein concentration in the supernatant was quantified using a DC Protein Assay Kit II (Bio-Rad). The samples (30 µg protein per lane) were subjected to 12% SDS-PAGE and electroblotted onto polyvinylidene fluoride (PVDF) membranes (Millipore) and then incubated with rabbit polyclonal antibody for 2 h at room temperature. The antigenic peptides (HSP70, CATENAGE-



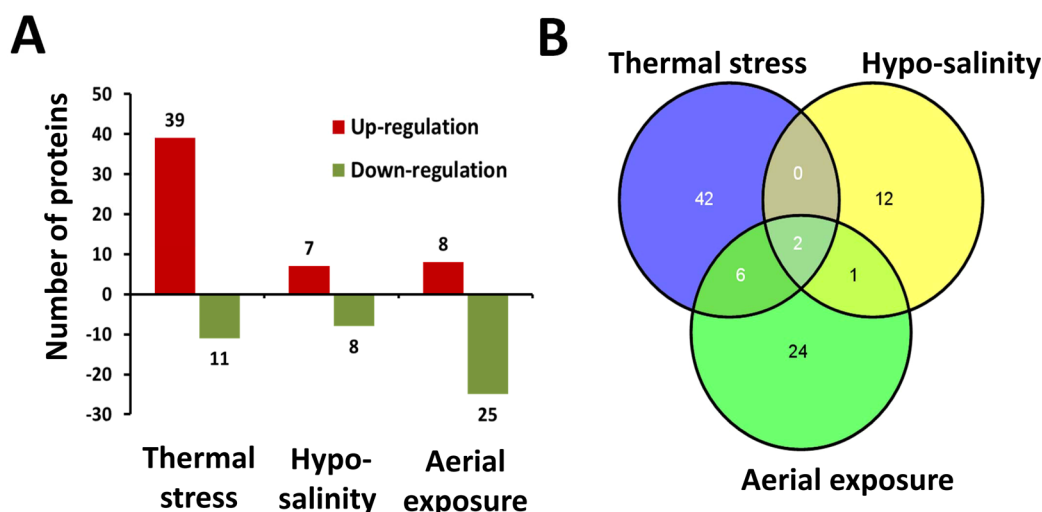


**Figure 1.** Number of differentially expressed proteins (A) and a Venn diagram showing the common and unique expressed proteins in response to the three stressors (B).

KLQPGDK; Cystatin B, CGGLSGAKKADCET; Calmodulin, CFKVFDDKDGSGDISA) were synthesized by GenScript (Nanjing, China). An extra “C” was added to the N terminus to facilitate conjugation. The primary antibodies were raised in rabbits against keyhole limpet hemocyanin (KLH)-conjugated peptides. Then, the antibodies were affinity-purified by using a specific peptide as ligand. The polyclonal antiactin of rabbit antibody was purchased from Abcam (Cambridge, U.K.). The specificity of all antibodies was tested by preincubation with synthesized antigenic peptides. Membranes were then incubated with HRP (horseradish peroxidase)-conjugated mouse antirabbit IgG (Cell Signaling Technology, USA). Finally, the bands were visualized using a Chemiluminescence Detection Kit (Life Technology) and quantified using ImageJ 1.48. The relationship between the Western blotting and iTRAQ data was assessed with linear correlation using GraphPad Prism 6.01.

## RESULTS AND DISCUSSION

### Proteome Characterization

Analysis of the three biological replicates resulted in 28 335, 34 906, and 31 809 peptide spectra, which corresponded to 2309, 2536, and 2530 of proteins, respectively (Supplementary Table S1 in the Supporting Information). Overall, 3165 proteins were identified from 95 050 peptides among which 15 186 were unique, and the average coverage of the peptides matched was 27.7%. Only proteins that contained at least two peptides and that were detected in all three replicates were used in quantification, which included 2379 proteins. Blast2GO classified the proteins into three categories: biological processes (BP, 2116; 33.2%), cellular components (CC, 1820; 28.6%), and molecular functions (MF, 2433; 38.2%) (Supplementary Figure S1 and Table S2 in the Supporting Information). The terms of metabolic process (GO:0008152, 35.3%), cell (GO:0005623, 27.3%), and catalytic activity (GO:0003824, 35.0%) were the most significantly represented category in BP, CC, and MF, respectively. These results show overwhelming superiority of our workflow over the traditional 2-DE approach, which reported no more than 500 proteins or protein spots in this species.<sup>25,26</sup>

In total, 87 DEPs were detected, with 50 in the heat shock treatment, 15 in the hyposalinity treatment, and 33 in the aerial exposure treatment (Figure 1A; Tables 1–3). Our data revealed that only a small part of the oyster gill proteome (87/2379, 3.66%) was involved in the stress responses, reflecting low rates of protein turnover during oyster stress response. In general, protein turnover, referring to the continuous biogenesis and degradation of cellular proteins, could provide a necessary flux for metabolic regulation and adaptation.<sup>37,38</sup> Similarly, lower rates of protein turnover were also observed in the gills of the marine mussel *Mytilus edulis* exposed to metals and heat stress, which was thought to contribute to energy saving, thereby enhancing the survival possibility for the animals under stress.<sup>32</sup>

To address whether *C. gigas* utilizes common or specific responses to cope with different stresses, we constructed a Venn diagram, which showed that most of the DEPs did not overlap among the three stress treatments, strongly suggesting that specific responses could be mobilized to defend distinct stresses (Figure 1B, Supplementary Figure S2 in the Supporting Information). Only two DEPs were shared among the three treatments. The first was xanthine dehydrogenase/oxidase (XOR) with a 0.55- to 0.83-fold down-regulation after exposure to the three stressors. It was also the only DEP with the same expressional trend irregardless of the type of stress. XOR is a critical source of reactive oxygen species (ROS) because superoxide anion and hydrogen peroxide can be generated while catalyzing the oxidation of hypoxanthine and xanthine.<sup>39</sup> In the marine mussel, the XOR activity has been detected in the epithelial cells of various types of tissues, including digestive gland and gill.<sup>40</sup> Considering that ROS accumulation can result in oxidative stress and impairment of normal physiological activities such as immune defense and metabolism,<sup>41</sup> decreased XOR expression may contribute to alleviation of deleterious effects caused by stress-induced accumulation of ROS. The other DEP shared among the three stress treatments was a hypothetical protein (CGI\_10026433), containing one signal peptide at the N-terminal and an ependymin (Epd) domain.<sup>42</sup> Previous studies have demonstrated that Epd containing protein was upregulated in the brain of teleost fish upon cold shock and hypoxia.<sup>43,44</sup> Although the underlying mechanism is still unclear, Epd-containing protein could prevent apoptosis through reversing intracellular accumulation of calcium.<sup>45</sup> In *C.*

Table 1. Differentially Expressed Proteins in Response to Heat Shock

protein description	protein accession number	mean	SD	no. of peptides matched	Pfam
<b>Molecular Chaperones</b>					
stress-induced protein 1	EKC27012	19.01	4.38	64	Hsp20/alpha crystallin family
stress-induced protein 1	EKC27011	13.30	3.09	105	Hsp20/alpha crystallin family
heat shock protein beta-1	EKC40046	9.84	1.48	37	Hsp20/alpha crystallin family
stress-induced protein 1	EKC27013	9.54	1.32	59	Hsp20/alpha crystallin family
heat shock protein 68	EKC22243	6.86	1.72	159	Hsp70 protein
BAG family molecular chaperone regulator 4	EKC42633	6.67	1.27	24	WW domain; BAG domain
heat shock protein 70 B2	EKC30019	5.89	1.53	159	Hsp70 protein
heat shock protein 70 B2	EKC21713	2.61	0.49	102	Hsp70 protein
heat shock protein beta-1	EKC27576	2.48	0.41	281	Hsp20/alpha crystallin family
heat shock 70 kDa protein 12A	EKC23126	0.51	0.20	5	
alpha-crystallin B chain	EKC27067	2.00	0.02	6	Hsp20/alpha crystallin family
hypothetical protein CGI_10004063	EKC36540	2.15	1.09	76	heat shock protein 9/12
<b>Enzyme and Metabolism</b>					
tyramine beta-hydroxylase	EKC38551	2.60	0.96	5	copper type II ascorbate-dependent monooxygenase, N-terminal domain
S-adenosylmethionine synthetase isoform type-2	EKC34165	1.88	0.18	34	S-adenosylmethionine synthetase, N-terminal domain
xanthine dehydrogenase/oxidase	EKC27500	0.55	0.14	3	FAD binding domain in molybdopterin dehydrogenase; aldehyde oxidase and xanthine dehydrogenase, a/b hammerhead domain
S-adenosylmethionine synthetase isoform type-1	EKC34163	1.52	0.17	64	S-adenosylmethionine synthetase, N-terminal domain
S-adenosylmethionine synthetase isoform type-1	EKC20435	1.43	0.22	31	S-adenosylmethionine synthetase, N-terminal domain
betaine-homocysteine S-methyltransferase	EKC24976	1.65	0.14	10	homocysteine S-methyltransferase
Poly [ADP-ribose] polymerase 1	EKC34863	0.73	0.20	12	poly(ADP-ribose) polymerase and DNA-Ligase Zn-finger region; poly(ADP-ribose) polymerase catalytic domain
liver carboxylesterase 4	EKC36594	0.69	0.12	7	carboxylesterase family
sulfotransferase 1A1, partial	EKC23587	1.79	0.19	3	sulfotransferase domain
estrogen sulfotransferase	EKC25638	1.57	0.26	13	sulfotransferase domain
lactoylglutathione lyase	EKC29441	1.36	0.30	15	glyoxalase/bleomycin resistance protein/dioxygenase superfamily
fatty acyl-CoA hydrolase precursor, medium chain	EKC30807	1.70	0.25	7	carboxylesterase family
ribose-phosphate pyrophosphokinase 3, mitochondrial	EKC29408	1.33	0.39	13	N-terminal domain of ribose phosphate pyrophosphokinase; phosphoribosyl transferase domain
natterin-1	EKC17431	0.80	0.43	45	protein of unknown function (DUF3421)
apolipoprotein D	EKC24158	0.63	0.24	9	lipocalin-like domain
hypothetical protein CGI_10000662	EKC32177	2.63	1.52	2	NAD:arginine ADP-ribosyltransferase
<b>Innate Immunity</b>					
beta-1,3-glucan-binding protein	EKC20362	1.66	0.45	17	
cystatin-B	EKC27128	1.77	1.00	183	cystatin domain
CD82 antigen	EKC39255	1.74	0.41	9	tetraspanin family
metalloproteinase inhibitor 3	EKC34907	1.75	0.56	29	tissue inhibitor of metalloproteinase
serine protease inhibitor dipetalogastin	EKC37817	2.67	2.26	7	kazal-type serine protease inhibitor domain
<b>Cytoskeletal Organization</b>					
transforming acidic coiled-coil-containing protein 1	EKC27162	2.15	0.36	8	transforming acidic coiled-coil-containing protein
tubulin-specific chaperone D	EKC31146	0.61	0.03	2	tubulin folding cofactor D C terminal
<b>Ca<sup>2+</sup> Binding Protein</b>					
calmodulin	EKC24247	1.75	0.48	23	EF-hand domain
EF-hand calcium-binding domain-containing protein 6	EKC37810	2.10	0.64	13	EF-hand domain
hypothetical protein CGI_10002317	EKC22425	1.51	0.59	6	EF-hand, calcium binding motif

Table 1. continued

protein description	protein accession number	mean	SD	no. of peptides matched	Pfam
<b>Signaling Pathway</b>					
dual specificity mitogen-activated protein kinase kinase 5	EKC41485	0.66	0.21	8	RNA recognition motif; protein kinase domain
<b>Other or Unknown Protein</b>					
UBX domain-containing protein 4	EKC38919	1.56	0.25	14	zinc-finger double domain
hypothetical protein CGI_10006238	EKC20363	1.51	0.35	12	lipoprotein N-terminal domain; domain of unknown function (DUF1943); von Willebrand factor (vWF) type D domain
Williams-Beuren syndrome chromosomal region 27 protein	EKC31167	1.45	0.21	10	methyltransferase domain
hypothetical protein CGI_10018187	EKC36599	1.41	0.37	18	
uncharacterized protein C7orf63	EKC28743	0.73	0.21	6	
hypothetical protein CGI_10018147	EKC39729	0.68	0.21	6	B41 domain
hypothetical protein CGI_10025411	EKC27421	0.62	0.09	5	YHYH protein
protein lethal(2)essential for life	EKC40045	1.97	0.14	26	Hsp20/alpha crystallin family
hypothetical protein CGI_10019192	EKC41324	1.59	0.26	13	
proline-rich transmembrane protein 1	EKC23568	2.04	0.41	3	interferon-induced transmembrane protein
hypothetical protein CGI_10026433	EKC41815	1.82	0.70	19	ependymin

Table 2. Differentially Expressed Proteins in Response to Hyposalinity

protein description	protein accession no.	mean	SD	no. of peptides matched	Pfam
<b>Enzyme and Metabolism</b>					
3-demethylubiquinone-9 3-methyltransferase	EKC32717	2.55	0.62	13	methyltransferase domain
aminoacylase-1	EKC40392	0.65	0.09	3	peptidase family M20/M25/M4
renalase	EKC21368	0.70	0.22	8	NAD(P)-binding Rossmann-like domain
xanthine dehydrogenase/oxidase	EKC27500	0.65	0.12	3	FAD binding domain in molybdopterin dehydrogenase; aldehyde oxidase and xanthine dehydrogenase, a/b hammerhead domain
omega-crystallin	EKC40622	0.64	0.37	8	aldehyde dehydrogenase family
<b>Cytoskeletal Organization</b>					
doublecortin domain-containing protein 5	EKC26279	1.28	0.45	3	ricin-type beta-trefoil lectin domain
<b>Excellular Protein</b>					
anosmin-1	EKC27374	0.56	0.01	3	SEA domain; WAP-type (whey acidic protein) 'four-disulfide core'
collagen alpha-2(VIII) chain	EKC36664	2.81	1.58	5	C1q domain
<b>Signaling Pathway</b>					
neurogenic locus notch-like protein	EKC34843	1.42	0.37	6	EGF-like domain; MAM domain
<b>Innate Immunity</b>					
hypothetical protein CGI_10011252	EKC39754	0.72	0.51	2	tumor necrosis factor receptor (TNFR) domain
hypothetical protein CGI_10018363	EKC35710	0.61	0.04	19	C-type lectin
<b>Other or Unknown Protein</b>					
hypothetical protein CGI_10005753	EKC42379	1.75	1.07	9	
hypothetical protein CGI_10008416	EKC33545	0.54	0.29	16	claudin_2
hypothetical protein CGI_10026433	EKC41815	1.74	0.86	8	ependymin
60S ribosomal protein L15	EKC39905	1.45	0.21	33	

*gigas*, its expression was up-regulated by the heat shock and hyposalinity treatments but down-regulated by the aerial exposure treatment, reflecting the versatility of this protein in response to different stressors, but its possible role of antiapoptosis in the oyster needs confirmation.

GOEAST analysis detected 1, 4, and 12 enriched GO terms in the hyposalinity, heat shock, and aerial exposure treatment, respectively (Table 4). Specifically, only intracellular signal transduction (GO:0035556) was enriched in the hyposalinity treatment. Four functional categories [response to stress

Table 3. Differentially Expressed Proteins in Response to Aerial Exposure

protein description	protein accession no.	mean	SD	no. of peptides matched	Pfam
<b>Ion Channl/Binding Protein</b>					
calmodulin	EKC24247	0.78	0.26	23	EF-hand domain
calmodulin	EKC20234	0.74	0.45	91	EF-hand domain
calmodulin	EKC24243	0.73	0.38	105	EF-hand domain
sodium- and chloride-dependent GABA transporter ine	EKC20246	0.53	0.33	22	dienelactone hydrolase family; sodium:neurotransmitter symporter family
sodium/calcium exchanger 3	EKC29251	1.70	0.28	4	sodium/calcium exchanger protein;Calx-beta domain
zinc transporter 8	EKC35076	0.62	0.03	5	ation efflux family
EF-hand calcium-binding domain-containing protein 6	EKC37810	0.69	0.37	13	EF-hand domain
<b>Enzyme and Metabolism</b>					
xanthine dehydrogenase/oxidase	EKC27500	0.83	0.57	3	FAD binding domain in molybdopterin dehydrogenase; aldehyde oxidase and xanthine dehydrogenase, a/b hammerhead domain
3-demethylubiquinone-9 3-methyltransferase	EKC32717	2.36	0.78	13	methyltransferase domain
laccase-18	EKC20149	0.76	0.31	6	multicopper oxidase
natterin-3	EKC36293	2.68	1.96	96	protein of unknown function (DUF3421)
hypothetical protein CGI_10018739	EKC30060	0.61	0.24	5	kynurenine formamidase
<b>Growth and Reproduction</b>					
signal peptide, CUB and EGF-like domain-containing protein 3	EKC30186	0.59	0.07	54	GCC2 and GCC3
vitellogenin, partial	EKC30050	0.79	0.41	4	lipoprotein amino terminal region
<b>Innate Immunity</b>					
beta-1,3-glucan-binding protein	EKC20362	0.84	0.53	17	
<b>DNA Duplication and Protein Synthesis</b>					
core histone macro-H2A.1	EKC23242	0.80	0.24	21	core histone H2A/H2B/H3/H4; macro domain
histone H1.2	EKC36128	0.54	0.13	5	linker histone H1 and H5 family
60S ribosomal protein L21	EKC17829	0.61	0.03	2	ribosomal protein L21e
<b>Antioxidation</b>					
selenoprotein H	EKC30285	0.59	0.05	2	Rdx family
<b>Lipid Metabolism</b>					
apolipoprotein D	EKC24158	0.70	0.40	9	lipocalin-like domain
<b>Other or Unknown Protein</b>					
crumbs-like protein 2	EKC39756	0.77	0.25	12	EGF-like domain; GCC2 and GCC3
heat shock 70 kDa protein 12B	EKC40489	1.32	0.45	22	Hsp70 protein
hypothetical protein CGI_10006238	EKC20363	0.79	0.43	12	lipoprotein N-terminal domain; von Willebrand factor (vWF) type D domain
hypothetical protein CGI_10011416	EKC18705	0.77	0.44	6	
hypothetical protein CGI_10014468	EKC32050	0.80	0.51	9	von Willebrand factor (vWF) type D domain
hypothetical protein CGI_10014616	EKC18177	0.55	0.45	25	DM9
hypothetical protein CGI_10021716	EKC34734	2.93	0.43	4	
hypothetical protein CGI_10026431	EKC41813	0.63	0.43	55	ependymin
hypothetical protein CGI_10026433	EKC41815	0.82	0.38	19	ependymin
hypothetical protein CGI_10026436	EKC41818	0.71	0.29	21	ependymin
pregnancy zone protein	EKC20077	1.54	0.65	6	alpha-2-macroglobulin family; alpha-macro-globulin thiol-ester bond-forming region
proline-rich transmembrane protein 1	EKC23568	1.70	0.06	3	interferon-induced transmembrane protein
transmembrane protein 2	EKC23142	1.61	0.47	11	HSF-type DNA-binding; homeobox domain

(GO:0006950), response to stimulus (GO:0050896), transferase activity (GO:0016740), and response to biotic stimulus (GO:0009607)] were enriched in the heat shock treatment. The 12 enriched GO terms in the aerial exposure treatment covered many biological components and functions, but among them, the most notable are ion binding (GO:0043167), transporter activity (GO:0005215), transport (GO:0006810), DNA binding (GO:0003677), and extracellular region (GO:0005576). These results also support that different stressors can trigger distinct proteomic responses. The possible roles of these DEPs in stress responses are analyzed as follows.

### Heat Shock

The heat shock treatment elicited the largest number of DEPs, including 39 up-regulated and 11 down-regulated proteins (Table 1). These DEPs have been known to modulate many biological processes including protein folding (molecular chaperones or HSP family), enzyme and metabolism, immune response, cytoskeletal organization, Ca<sup>2+</sup> binding, signaling, and other functions. Notably, many of the heat-shock-induced proteins [e.g., stress-induced protein 1 (SIP1), HSP70, HSP- $\beta$ , and S-adenosylmethionine synthetase (MAT)] had several paralogs, which highlighted the large repertoire of proteins

Table 4. Distribution of Enriched Protein Pathways<sup>a</sup>

category	term (GO number)	count	P value
<b>Thermal Stress</b>			
BP	response to stress (GO:0006950)	5	0.0020
BP	response to stimulus (GO:0050896)	6	0.0497
MF	transferase activity (GO:0016740)	11	0.0020
BP	response to biotic stimulus (GO:0009607)	1	0.0418
<b>Hyposalinity</b>			
BP	intracellular signal transduction (GO:0035556)	1	0.0126
<b>Aerial Exposure</b>			
MF	transporter activity (GO:0005215)	6	0.0006
BP	transport (GO:0006810)	6	0.0219
BP	localization (GO:0051179)	6	0.0219
BP	establishment of localization(GO:0051234)	6	0.0219
BP	response to biotic stimulus(GO:0009607)	1	0.0285
MF	DNA binding (GO:0003677)	3	0.0198
CC	extracellular region (GO:0005576)	1	0.0062
CC	chromosome (GO:0005694)	2	0.0121
MF	calcium ion binding (GO:0005509)	5	0.0011
MF	ion binding (GO:0043167)	7	0.0011
MF	cation binding (GO:0043169)	7	0.0011
MF	metal ion binding (GO:0046872)	4	0.0011

<sup>a</sup>Only the terms with a corrected *P* value <0.05 were considered to be enriched. Abbreviation: BP, biological process; CC, cellular component; and MF, molecular function.

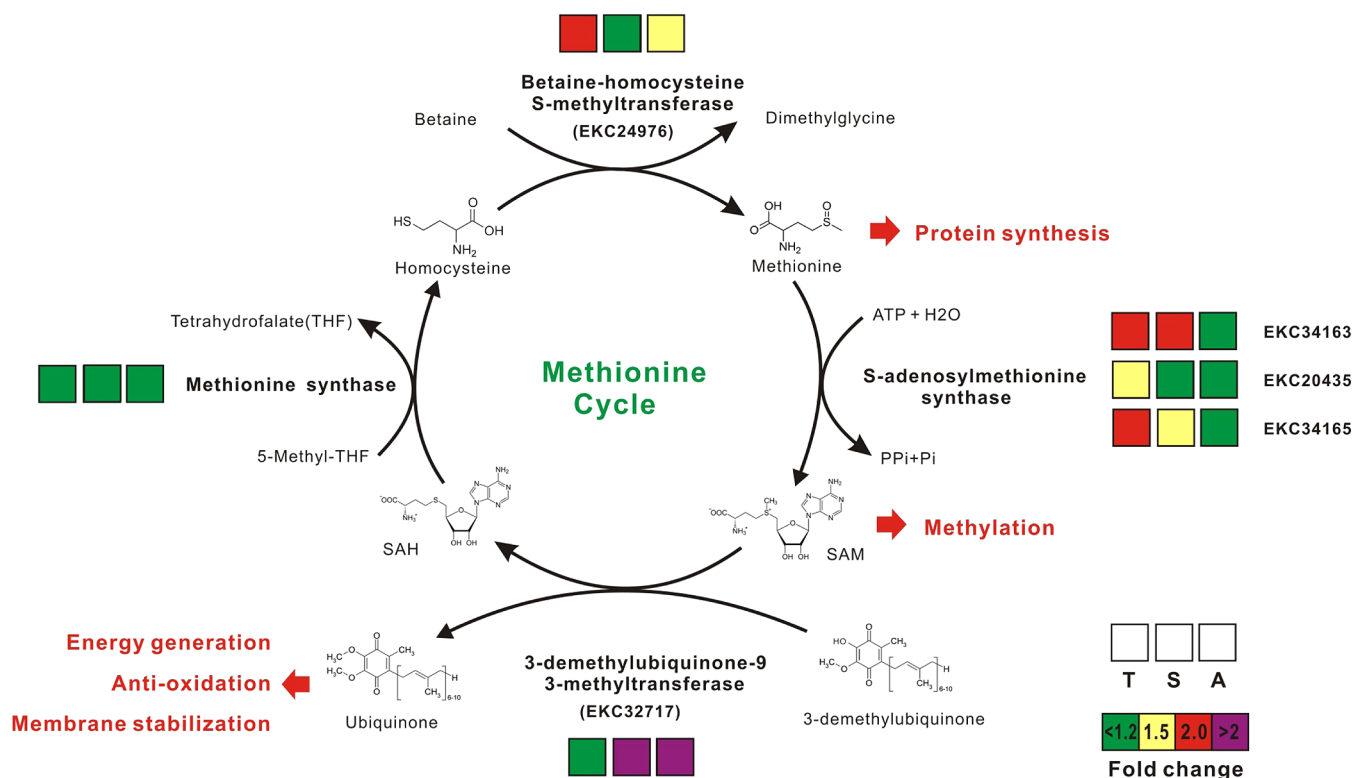


**Figure 2.** Involvement of the methionine cycle in oyster stress response. There are four metabolites (homocysteine, methionine, SAM, and SAH) in the methionine cycle. The enzymes involved in this cycle are significantly regulated upon exposure to the three stressors, with the fold change of these enzymes indicated by a color. Four colors (green, yellow, red, and purple) represent different fold change (<1.2, 1.2–1.5, 1.5–2.0, >2.0), respectively. SAM, *S*-adenosyl-*L*-methionine; SAH, *S*-adenosylhomocysteine; ATP, adenosine triphosphate; P<sub>Pi</sub>, inorganic pyrophosphate; Pi, inorganic phosphate; T, thermal stress; S, hyposalinity; A, aerial exposure.

available for use to cope with thermal stress in *C. gigas*. Significantly, our proteomic analysis showed that the abundance of 11 HSP family members was dramatically induced after the stress exposure, including SIP1, HSP beta-1,

HSP68, HSP70 B2, alpha-crystallin B, and HSP9/12, providing the first evidence that many of these molecular chaperons are active, strongly corroborating their crucial role in increasing thermal tolerance through stabilizing protein conformation,



preventing unwanted protein aggregation and aiding transporting proteins across membranes.<sup>46</sup> Also, previous studies have shown that the thermal limits of oysters were correlated with the expression level of HSP family members, especially HSP70.<sup>3,47</sup> Strikingly, three paralogs of SIP1 containing the typical HSP20 domain had the highest fold increase (9.5- to 19-fold). To our knowledge, this is the first report of high expression of SIP 1s upon heat shock in oysters. Although the exact role of SIPs is still unknown, there is evidence that proteins with the HSP20 domain can stabilize cytoskeleton and protect against oxidative stress,<sup>48</sup> providing a promising candidate for further investigation. Although many HSPs can prevent protein denature by thermal stress, their accumulation has been reported to inflict energetic cost through depleting adenylate energy charge and mantle glycogen store in the spawning oysters, thus compromising their physiological and immune health.<sup>49</sup> To limit the potentially deleterious effect of HSPs, an HSP suppressor, BAG family molecular chaperone regulator 4 (BAG4),<sup>57</sup> increased by 6.67-fold in the heat shock treatment, strongly suggesting concerted regulation in maintaining cellular hemostasis *in vivo*.<sup>50</sup>

Alternation of metabolism is tightly associated with physiological adaptation. Among the DEPs responsive to the heat shock were 16 enzymes implicated in amino acid and lipid metabolism or other catalytic activities. Interestingly, four essential enzymes involved in the methionine cycle, including a betaine-homocysteine *S*-methyltransferase (BHMT, EC:2.1.1.5) and three isoforms of *S*-adenosylmethionine synthetase (also known as methionine adenosyltransferase MAT, EC2.5.1.6), were up-regulated by 1.43- to 1.88-fold (Figure 2). In the methionine cycle, BHMT catalyzes the conversion of homocysteine to methionine using betaine as the methyl donor.<sup>51</sup> In addition to its role in protein synthesis, methionine can aid the synthesis of *S*-adenosylmethionine (SAM) by joining ATP. As the predominant methyl donor *in vivo*, there is evidence that SAM may increase thermal tolerance via a variety of possible mechanisms, including (1) repairing the lipid membranes through synthesizing phospholipids, the major component of all cell membranes;<sup>49</sup> (2) epigenetic regulating stress-responsive gene expression through DNA and histone methylation;<sup>52</sup> (3) regulating the function of HSPs by methylation;<sup>53</sup> and (4) increasing reduced/oxidized glutathione ratio and potentiating superoxide dismutase activity.<sup>54</sup> Meanwhile, lipid metabolism might also be involved in the heat shock response, as indicated by the differential expression of two lipid metabolism related proteins, fatty acyl-CoA hydrolase (ACH) precursor, and apolipoprotein D (APO-D). Acute heat shock can damage lipid membranes by either changing the physical state of membranes or causing oxidative stress.<sup>55,56</sup> ACH can catalyze palmitate biosynthesis that is a typical fatty acid of lipid membrane. Therefore, increased expression of ACH might contribute to repairing lipid membrane that were the damaged by heat shock. However, APO-D, which is responsible for transporting lipids and other small hydrophobic molecules for metabolism,<sup>57</sup> was down-regulated by the heat shock, but the exact role of this protein in the heat response is still unknown.

In marine mussels *Mytilus* spp., acute temperature stress could induce DNA damage and apoptosis in the hemocytes.<sup>56</sup> Correspondingly, our results showed that several enzymes implicated in these processes altered their abundance in response to the heat shock in the oyster gills. For example, lactoylglutathione lyase (EC 4.4.1.5, LGL, also known as

glyoxalase I) is responsible for detoxifying methylglyoxal that could induce apoptosis.<sup>58</sup> Thus, up-regulation of LGL could help to prevent the potential damage and cellular toxicity caused by methylglyoxal. Ribose-phosphate pyrophosphokinase (EC 2.7.6.1., PRS) can convert ribose 5-phosphate into phosphoribosyl pyrophosphate (PRPP), which is a key component in numerous biosynthesis pathways, including *de novo* synthesis of purines and pyrimidines, conversion of nucleotide cytidine triphosphate (CTP), adenosine triphosphate (ATP), or guanosine triphosphate (GTP).<sup>59</sup> Obviously, an increase in PRPP synthesis might contribute to the repair of heat shock caused DNA damage. Meanwhile, PRPP has also been demonstrated to be an intermediate chemical in the synthesis of nicotinamide adenine dinucleotide (NAD).<sup>60</sup> In addition, NAD can be converted into nicotinamide, a process catalyzed by the enzyme arginine ADP-ribosyltransferase (EC 2.4.2.31, ART1).<sup>61</sup> The expression of this enzyme increased by 2.63-fold after the heat shock in our study. In mammalian cells, nicotinamide is capable of preventing oxidative stress-induced apoptosis through decreasing constitutive activity of NF- $\kappa$ B and increasing intracellular levels of GAPDH.<sup>62</sup> Meanwhile, the abundance of poly(ADP-ribose) polymerase (PARP) decreased by 0.73-fold. Because previous studies have revealed the dual roles of PARP in repairing DNA and inducing programmed cell death,<sup>63</sup> down-regulation of PARP might reflect the demand to balance between DNA repair and apoptosis.

A number of immune-related proteins including beta-1,3-glucan-binding protein ( $\beta$ -GBP), CD82 antigen, cystatin-B (CSTB), metalloproteinase inhibitor 3 (TIMP-3), and serine protease inhibitor dipetalogastin (Dip) were significantly up-regulated, suggesting that heat shock could trigger a rapid and intense inflammatory response in the oyster. Previous studies have demonstrated that high temperature could impair immunity due to the reduced ability of phagocytosis to kill bacteria, consequently increasing the susceptibility to opportunistic infection.<sup>64</sup> Meanwhile, bacterial pathogens secrete proteases to injure the host cells during infection; therefore, protease inhibitors including CSTB and TIMP-3 can prevent pathogen attack and increase resistance against pathogens in oysters.<sup>65</sup> Taken together, up-regulation of immune regulatory proteins and proteinase inhibitors could compensate the reduced level of innate immunity caused by heat shock in the oyster.

In addition, heat stress affects the abundance of proteins that are involved in  $\text{Ca}^{2+}$  binding, cytoskeletal organization, signaling pathway, and other functions, displaying that thermal stress has caused complex effects on various physiological activities. For example, among the DEPs are three  $\text{Ca}^{2+}$  binding proteins [one calmodulin (CaM) and two EF-hand calcium-binding domain-containing proteins (CaBP)]. These proteins have been reported to control  $\text{Ca}^{2+}$ -triggered signaling via regulating the intracellular  $\text{Ca}^{2+}$  concentration,<sup>66</sup> which indicated that  $\text{Ca}^{2+}$ -triggered signaling might have been involved in the oyster's thermal response.

### Hyposalinity

Among the three tested stressors, hyposalinity elicited the smallest number of DEPs (Table 2), possibly due to the oyster's strong euryhaline adaptation.<sup>22</sup> Nevertheless, our results showed that hyposalinity affected proteins mainly involved in enzyme and metabolism, cytoskeleton, extracellular matrix, signaling pathway, innate immunity, and other unknown

functions. Several enzymes were up-regulated [3-demethylubiquinone-9 3-methyltransferase (UbiG)] or down-regulated [XOR (discussed already), aminoacylase-1 (ACY-1), renalase, and omega-Crystallin]. Interestingly, UbiG (EC 2.1.1.64), which can convert demethylubiquinone into ubiquinone using SAM as a methyl donor, was greatly up-regulated by the hyposalinity (2.55 fold) and aerial exposure (2.36 fold) but not by heat shock (Figure. 2). Ubiquinone is an essential compound of the electron transport chain (ETC) to generate energy and can also act as an antioxidant to inhibit both the initiation and propagation of lipid and protein oxidation.<sup>67</sup> Meanwhile, a recent study also showed that ubiquinone biosynthesis was markedly activated upon hyposalinity challenge in bacteria, and consequently accumulation of ubiquinone could enhance mechanical membrane stabilization to withstand osmotic stress.<sup>68</sup> This evidence indicates that ubiquinone may play a crucial role in osmotic protection in the Pacific oyster, although ubiquinone has not been reported to function in osmotic regulation in any marine invertebrate or vertebrate. This hypothesis can be tested by measuring the metabolome. ACY1 (EC 3.5.14), another hyposalinity responsive DEP, participates in intracellular protein catabolism in mammals through hydrolyzing *N*-acetyl amino acids (NAAs) into free amino acids, and NAAs can modify *N*-acetylation of proteins to protect cells from proteolysis.<sup>69</sup> Therefore, down-regulation of ACY1 may favor the accumulation of NAAs and consequently enhance the resistance of proteins to osmotic stress-induced degradation in the Pacific oyster.

Osmotic stress responses are a series of coordinated physiological functions involving hormonal signaling. Catecholamine (CA) is one of the hormones to modulate the proximal tubular sodium transport in the mammalian kidney.<sup>70</sup> In oysters, hyposalinity was reported to elicit a significant increase in the expression of two circulating CAs, noradrenaline (NA) and dopamine (DA), whose concentrations peaked at 12 h and lasted up to 72 h of poststress.<sup>71</sup> In contrast, our results showed that hyposalinity could reduce the expression of renalase, which is a secreted amine oxidase to metabolize circulating CAs,<sup>70</sup> indicating that the oyster could reduce the degradation rate of CAs to enhance osmotic stress tolerance.

Adjustments of cell volume require cytoskeletal rearrangement and membrane modification, which is pivotal for osmotic regulation.<sup>72</sup> The double cortin domain-containing protein 5 (DCDC5) has been reported to facilitate tubulin binding and enhance microtubule polymerization.<sup>73</sup> Moreover, a knock-down of DCDC5 in the HeLa cells also revealed its important role in mediating dynein-dependent transport of vesicles.<sup>74</sup> In the Pacific oyster, we detected the up-regulation of DCDC5 after hyposalinity exposure, suggesting that this protein may be involved in osmotic regulation through cytoskeletal adjustment and vesicles transport. Moreover, hyposalinity also has profound effects on growth and immunity. For example, among our hyposalinity responsive DEPs are two extracellular matrix proteins, collagen alpha-2(VIII) chain and anosmin-1. Collagen could deposit on cell surface and disturb tissue growth and repair,<sup>75</sup> while anosmin-1 could enhance FGF activity by promoting FGF8-FGFR1 complex formation.<sup>76</sup> A previous study showed that reduced salinity (~15‰) could significantly delay the growth of oyster larvae,<sup>77</sup> and thus either up-regulation of collagen alpha-2(VIII) or down-regulation of anosmin-1 might indicate that hyposalinity caused growth arrest in adult oysters. Hyposalinity might also impair immune responses, as shown by the down-regulation of tumor necrosis

factor receptor (TNFR, hypothetical protein CGI\_10011252) and C-type lectin (hypothetical protein CGI\_10018363) in the gills, both of which have been reported to be involved in the immune responses in oysters.<sup>78</sup>

### Aerial Exposure

Exposure to air can be considered as an extreme osmotic stress due to the complete lack of ions and water in the extracellular environment;<sup>4</sup> therefore, oysters are required to regulate intercellular concentration of ions and other osmolytes.<sup>16</sup> Although a previous study found that the concentrations of various intracellular ions (i.e., Ca<sup>2+</sup> and Na<sup>+</sup>) would drop when external ion concentrations decrease in oysters, the mechanisms remains unclear.<sup>79</sup> Interestingly, our results showed that several ion channels and transporters, the direct executors of osmotic homeostasis, were altered under aerial exposure, including up-regulation in sodium/calcium exchanger 3 (NCX3) and down-regulation of sodium- and chloride-dependent GABA transporter (GAT) and zinc transporter 8 (ZnT8) (Table 3). GAT can transport two sodium ions together with GABA from the cell, and ZnT8 is responsible for the high level of zinc accumulation in the cell.<sup>80</sup> Thus, aerial exposure may decrease intracellular ion concentration via down-regulation of the two transporters. Meanwhile, NCX3, a cation membrane channel protein, can pump Ca<sup>2+</sup> out of the cell and reduce the concentration of cellular Ca<sup>2+</sup>.<sup>81</sup> Thus, up-regulation of NCX3 also favored the decrease in intercellular Ca<sup>2+</sup> concentration for oysters exposed to air. Moreover, four Ca<sup>2+</sup>-binding proteins including three paralogs of CaM and one CaBP6 all decreased in expression upon aerial exposure, strongly indicating that desiccation stress not only resulted in a decrease in intercellular Ca<sup>2+</sup> concentration but also limited Ca<sup>2+</sup> signaling-related physiological activities. Considering that the intracellular Ca<sup>2+</sup> concentration is tightly coupled to many cell activities such as proliferation, development, contraction, secretion, and so on,<sup>66</sup> decreasing Ca<sup>2+</sup> and Ca<sup>2+</sup>-related binding protein concentrations would likely reduce many physiological activities and direct the limited resources to vital functions, such as synthesis of ubiquinone.

Our proteomic data also showed that many physiological activities were extensively suppressed because the expression levels of many proteins implicated in metabolism, immune response, DNA duplication and protein synthesis, growth, and antioxidation were all down-regulated (Table 3). All metabolism-related proteins such as XOR, APO-D, and kynurenine formamidase (KFase, EC 3.5.1.9, hypothetical protein CGI\_10018739, involvement in the aerobic degradation of tryptophan or kynurenine pathway<sup>82</sup>) were down-regulated under aerial exposure except for up-regulation of UbiG, highlighting that aerial exposure could activate the ubiquinone defense pathway similar to hyposalinity and reduce the ROS generation and metabolism of lipid and amino acids as well. Aerial exposure might also affect the growth, as shown by the down-regulation of signal peptide CUB-EGF-like domain-containing protein 3 (SCUBE3). SCUBE3 is an endogenous ligand that activates the TGF- $\beta$  receptor signaling. It also acts as a FGF coreceptor to augment FGF8 signaling, which modulates cell growth and differentiation in mammals.<sup>83</sup> Moreover, two immune defense-related proteins,  $\beta$ -GBP and laccase-18, were down-regulated under the aerial exposure.  $\beta$ -GBP is an important PRR in oyster innate immunity as previously mentioned, and laccase constituted innate antibacterial immune response against pathogen infection in oysters, revealing that

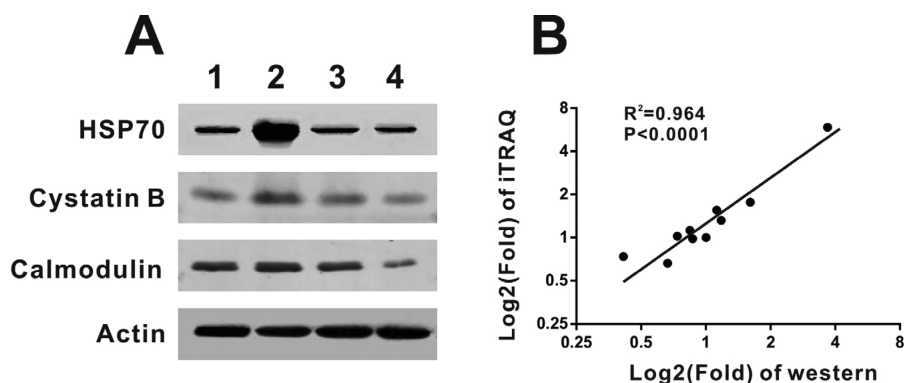


**Figure 3.** Validation of several differentially expressed proteins (HSP90, Cystatin B, and Calmodulin) by Western blotting with actin as reference. Lane 1, control; Lane 2, thermal stress; Lane 3, hyposalinity; Lane 4, aerial exposure.

aerial exposure compromises the innate immune defense.<sup>84</sup> In addition, aerial exposure also suppressed DNA duplication and protein synthesis because three proteins including histone 1.2, core histone macro-H2A.1, and 60S ribosomal protein L21 were all down-regulated during aerial exposure. Taken together, our data indicated that aerial exposure resulted in extensive reduced physiological activities, reflecting energy conservation and redistribution of available resources to fuel stress responses.

#### Validation and Correlation of Protein Expression by Western Blotting

To validate the protein abundance quantified by iTRAQ, we determined the expression level of three candidate DEPs, including HSP90, Cystatin B, and Calmodulin, by Western blotting with actin as the reference. Obviously, the bands of HSP90 and Cystatin B had a greater intensity upon thermal stress than that of control, and Calmodulin was significantly decreased after aerial exposure (Figure 3A). Correlation analysis showed high consistency between the iTRAQ data and Western blotting data ( $P < 0.0001$ , Figure 3B). Although it has been reported that the fold change determined by iTRAQ may be underestimated compared with other methods such as the blue native gel or label-free method,<sup>85</sup> our Western blotting results were highly consistent with the iTRAQ results, demonstrating the high reproducibility of our proteomics workflow.

#### CONCLUDING REMARKS

This is the first application of high-throughput LC-MS/MS to compare the proteomic responses of the *C. gigas* gills to three common physical stressors, demonstrating the great utility of our workflow in determining the molecular basis of adaptation to environment stresses and climate change. Our results have not only confirmed the functions of several proteins or genes identified previously using the individual gene or transcriptomics approaches but also revealed some novel important physiological adaptations. Reduction of XOR level appears to be a common response of the gills to the three stressors. The oyster gills can employ different defense mechanisms to cope with different stressors. Specifically, enhancing SAM production and HSP synthesis can contribute to promoting thermal tolerance; increasing ubiquinone synthesis plays a dual role in withstanding osmotic and desiccation stresses; whereas suppressing many physiological activities and decreasing intercellular ion concentration can be the most important mechanism to cope with aerial exposure in the Pacific oyster.

#### ASSOCIATED CONTENT

##### Supporting Information

Supplementary Table S1. Identification and relative abundance of gill proteins in *C. gigas*. Supplementary Table S2. The detailed GO terms for the *C. gigas* gill proteome. Supplementary Figure S1. The number of proteins in enriched GO categories in the oyster gill proteome, obtained from DAVID with a corrected  $P < 0.05$ . Supplementary Figure S2. The heat map showing the expression profile of differentially expressed proteins in response to three stressors. This material is available free of charge via the Internet at <http://pubs.acs.org>.

#### AUTHOR INFORMATION

##### Corresponding Authors

\*Jian-Wen Qiu: Tel: +852-34117055. Fax: +852-34115995. E-mail: [qiujiw@hkbu.edu.hk](mailto:qiujiw@hkbu.edu.hk).

\*Ziniu Yu: Tel/Fax: +86 20 8910-2507. E-mail: [carlzyu@scsio.ac.cn](mailto:carlzyu@scsio.ac.cn).

##### Author Contributions

<sup>¶</sup>Yang Zhang and Jin Sun contributed equally to this paper.

##### Notes

The authors declare no competing financial interest.

#### ACKNOWLEDGMENTS

This study was supported by the Joint Funds of NSFC-Guangdong (no. U1201215), the National Basic Research Program of China (no. 2010CB126404), and University Grant Committee of Hong Kong (no. GRF 261312). The mass spectrometry was performed in Instrumental Analysis & Research Center, Sun Yat-Sen University. We thank Miss Ling Fang for assistance with the mass spectrometry.

#### REFERENCES

- (1) Doney, S. C.; Fabry, V. J.; Feely, R. A.; Kleypas, J. A. Ocean acidification: the other CO<sub>2</sub> problem. *Ann. Rev. Mar. Sci.* **2009**, *1*, 169–192.
- (2) Durack, P. J.; Wijffels, S. E.; Matear, R. J. Ocean salinities reveal strong global water cycle intensification during 1950 to 2000. *Science* **2012**, *336*, 455–458.
- (3) Farcy, E.; Voiseux, C.; Lebel, J. M.; Fievet, B. Transcriptional expression levels of cell stress marker genes in the Pacific oyster *Crassostrea gigas* exposed to acute thermal stress. *Cell Stress Chaperones* **2009**, *14*, 371–380.
- (4) Berger, V. J.; Kharazova, A. D. Mechanisms of salinity adaptations in marine molluscs. *Hydrobiologia* **1997**, *355*, 115–126.



- (5) Pierce, S. K.; Amende, L. M. Control mechanisms of amino acid-mediated cell-volume regulation in salinity-stressed mollusks. *J. Exp. Zool.* **1981**, *215*, 247–257.
- (6) Hoyaux, J.; Gilles, R.; Jeuniaux, C. Osmoregulation in molluscs of the intertidal zone. *Comp. Biochem. Physiol., Part A* **1976**, *53*, 361–365.
- (7) Guo, X. Use and exchange of genetic resources in molluscan aquaculture. *Rev. Aquaculture* **2009**, *1*, 251–259.
- (8) Zhang, G.; Fang, X.; Guo, X.; Li, L.; Luo, R.; Xu, F.; Yang, P.; Zhang, L.; Wang, X.; Qi, H.; Xiong, Z.; Que, H.; Xie, Y.; Holland, P. W.; Paps, J.; Zhu, Y.; Wu, F.; Chen, Y.; Wang, J.; Peng, C.; Meng, J.; Yang, L.; Liu, J.; Wen, B.; Zhang, N.; Huang, Z.; Zhu, Q.; Feng, Y.; Mount, A.; Hedgecock, D.; Xu, Z.; Liu, Y.; Domazet-Lošo, T.; Du, Y.; Sun, X.; Zhang, S.; Liu, B.; Cheng, P.; Jiang, X.; Li, J.; Fan, D.; Wang, W.; Fu, W.; Wang, T.; Wang, B.; Zhang, J.; Peng, Z.; Li, Y.; Li, N.; Chen, M.; He, Y.; Tan, F.; Song, X.; Zheng, Q.; Huang, R.; Yang, H.; Du, X.; Chen, L.; Yang, M.; Gaffney, P. M.; Wang, S.; Luo, L.; She, Z.; Ming, Y.; Huang, W.; Huang, B.; Zhang, Y.; Qu, T.; Ni, P.; Miao, G.; Wang, Q.; Steinberg, C. E.; Wang, H.; Qian, L.; Liu, X.; Yin, Y. The oyster genome reveals stress adaptation and complexity of shell formation. *Nature* **2012**, *490*, 49–54.
- (9) Cho, E. S.; Jeong, H. D. Effect of environmental impact to molecular expression of heat-shock protein (HSP70) in oyster *Crassostrea gigas* from Gamak bay, Korea. *J. Environ. Biol.* **2012**, *33*, 609–615.
- (10) Kawabe, S.; Yokoyama, Y. Role of hypoxia-inducible factor alpha in response to hypoxia and heat shock in the Pacific oyster *Crassostrea gigas*. *Mar. Biotechnol.* **2012**, *14*, 106–119.
- (11) Meistertzheim, A. L.; Tanguy, A.; Moraga, D.; Thebault, M. T. Identification of differentially expressed genes of the Pacific oyster *Crassostrea gigas* exposed to prolonged thermal stress. *FEBS J.* **2007**, *274*, 6392–6402.
- (12) Toyohara, H.; Ikeda, M.; Goto, C.; Sawada, H.; Hosoi, M.; Takeuchi, K.; Hayashi, I.; Imamura, S.; Yamashita, M. Osmo-responsive expression of oyster amino acid transporter gene and analysis of the regulatory region involved. *Fisheries Sci.* **2005**, *71*, 465–470.
- (13) Hosoi, M.; Shinzato, C.; Takagi, M.; Hosoi-Tanabe, S.; Sawada, H.; Terasawa, E.; Toyohara, H. Taurine transporter from the giant Pacific oyster *Crassostrea gigas*: function and expression in response to hyper- and hypo-osmotic stress. *Fisheries Sci.* **2007**, *73*, 385–394.
- (14) Eierman, L. E.; Hare, M. P. Transcriptomic analysis of candidate osmoregulatory genes in the eastern oyster *Crassostrea virginica*. *BMC Genomics* **2014**, *15*, 503.
- (15) Lang, R. P.; Bayne, C. J.; Camara, M. D.; Cunningham, C.; Jenny, M. J.; Langdon, C. J. Transcriptome profiling of selectively bred Pacific Oyster *Crassostrea gigas* families that differ in tolerance of heat shock. *Mar. Biotechnol.* **2009**, *11*, 650–668.
- (16) Meng, J.; Zhu, Q. H.; Zhang, L. L.; Li, C. Y.; Li, L.; She, Z. C.; Huang, B. Y.; Zhang, G. F. Genome and transcriptome analyses provide insight into the euryhaline adaptation mechanism of *Crassostrea gigas*. *PLoS One* **2013**, *8* (3), e58563.
- (17) Lockwood, B. L.; Sanders, J. G.; Somero, G. N. Transcriptomic responses to heat stress in invasive and native blue mussels (genus *Mytilus*): molecular correlates of invasive success. *J. Exp. Biol.* **2010**, *213*, 3548–3558.
- (18) Lockwood, B. L.; Somero, G. N. Transcriptomic responses to salinity stress in invasive and native blue mussels (genus *Mytilus*). *Mol. Ecol.* **2011**, *20*, 517–529.
- (19) Clark, M. S.; Thorne, M. A. S.; Amaral, A.; Vieira, F.; Batista, F. M.; Reis, J.; Power, D. M. Identification of molecular and physiological responses to chronic environmental challenge in an invasive species: the Pacific oyster, *Crassostrea gigas*. *Ecol. Evol.* **2013**, *3*, 3283–3297.
- (20) Feder, M. E.; Walsler, J. C. The biological limitations of transcriptomics in elucidating stress and stress responses. *J. Evolution Biol.* **2005**, *18*, 901–910.
- (21) Gstaiger, M.; Aebersold, R. Applying mass spectrometry-based proteomics to genetics, genomics and network biology. *Nat. Rev. Genet.* **2009**, *10*, 617–627.
- (22) Tomanek, L. Environmental proteomics: Changes in the proteome of marine organisms in response to environmental stress, pollutants, infection, symbiosis, and development. *Annu. Rev. Mar. Sci.* **2011**, *3*, 373–399.
- (23) Buckley, B. A.; Gracey, A. Y.; Somero, G. N. The cellular response to heat stress in the goby *Gillichthys mirabilis*: a cDNA microarray and protein-level analysis. *J. Exp. Biol.* **2006**, *209*, 2660–2677.
- (24) Muralidharan, S.; Thompson, E.; Raftos, D.; Birch, G.; Haynes, P. A. Quantitative proteomics of heavy metal stress responses in Sydney rock oysters. *Proteomics* **2012**, *12*, 906–921.
- (25) Tomanek, L.; Zuzow, M. J.; Ivanina, A. V.; Beniash, E.; Sokolova, I. M. Proteomic response to elevated PCO<sub>2</sub> level in eastern oysters, *Crassostrea virginica*: evidence for oxidative stress. *J. Exp. Biol.* **2011**, *214*, 1836–1844.
- (26) Dineshran, R.; Wong, K. K. W.; Xiao, S.; Yu, Z. N.; Qian, P. Y.; Thiyagarajan, V. Analysis of Pacific oyster larval proteome and its response to high-CO<sub>2</sub>. *Mar. Pollut. Bull.* **2012**, *64* (10), 2160–2167.
- (27) Corporeau, C.; Tamayo, D.; Pernet, F.; Quééré, C.; Madec, S. Proteomic signatures of the oyster metabolic response to herpesvirus OsHV-1  $\mu$ Var infection. *J. Proteomics* **2014**, *109*, 176–187.
- (28) Wu, W. W.; Wang, G. H.; Baek, S. J.; Shen, R. F. Comparative study of three proteomic quantitative methods, DIGE, cICAT, and iTRAQ using 2D gel- or LC-MALDI TOF/TOF. *J. Proteome Res.* **2006**, *5*, 651–658.
- (29) Ross, P. L.; Huang, Y. L. N.; Marchese, J. N.; Williamson, B.; Parker, K.; Hattan, S.; Khainovski, N.; Pillai, S.; Dey, S.; Daniels, S.; Purkayastha, S.; Juhasz, P.; Martin, S.; Bartlett-Jones, M.; He, F.; Jacobson, A.; Pappin, D. J. Multiplexed protein quantitation in *Saccharomyces cerevisiae* using amine-reactive isobaric tagging reagents. *Mol. Cell. Proteomics* **2004**, *3*, 1154–1169.
- (30) Chong, P. K.; Gan, C. S.; Pham, T. K.; Wright, P. C. Isobaric tags for relative and absolute quantitation (iTRAQ) reproducibility: Implication of multiple injections. *J. Proteome Res.* **2006**, *5*, 1232–1240.
- (31) Gan, C. S.; Chong, P. K.; Pham, T. K.; Wright, P. C. Technical, experimental, and biological variations in isobaric tags for relative and absolute quantitation (iTRAQ). *J. Proteome Res.* **2007**, *6*, 821–827.
- (32) Tomanek, L.; Zuzow, M. J. The proteomic response of the mussel congeners *Mytilus galloprovincialis* and *M. trossulus* to acute heat stress: implications for thermal tolerance limits and metabolic costs of thermal stress. *J. Exp. Biol.* **2010**, *213*, 3559–3574.
- (33) Sun, J.; Mu, H. W.; Zhang, H. M.; Chandramouli, K. H.; Qian, P. Y.; Wong, C. K. C.; Qiu, J. W. Understanding the Regulation of Estivation in a Freshwater Snail through iTRAQ-Based Comparative Proteomics. *J. Proteome Res.* **2013**, *12*, 5271–5280.
- (34) Hao, P.; Qian, J.; Ren, Y.; Sze, S. K. Electrostatic repulsion-hydrophilic interaction chromatography (ERLIC) versus strong cation exchange (SCX) for fractionation of iTRAQ-labeled peptides. *J. Proteome Res.* **2011**, *10*, 5568–5574.
- (35) Zheng, Q.; Wang, X. J. GOEAST: a web-based software toolkit for Gene Ontology enrichment analysis. *Nucleic Acids Res.* **2008**, *36*, W358–W363.
- (36) Finn, R. D.; Bateman, A.; Clements, J.; Coggill, P.; Eberhardt, R. Y.; Eddy, S. R.; Heger, A.; Hetherington, K.; Holm, L.; Mistry, J.; Sonnhammer, E. L.; Tate, J.; Punta, M. Pfam: the protein families database. *Nucleic Acids Res.* **2014**, *42*, D222–D230.
- (37) Hawkins, A. J. S.; Rusin, J.; Bayne, B. L.; Day, A. J. The metabolic physiological-basis of genotype-dependent mortality during copper exposure in *Mytilus-Edulis*. *Mar. Environ. Res.* **1989**, *28*, 253–257.
- (38) Hawkins, A. J. S.; Wilson, I. A.; Bayne, B. L. Thermal responses reflect protein turnover in *Mytilus edulis* L. *Funct. Ecol.* **1987**, *1*, 339–351.
- (39) Tarpey, M. Xanthine oxidoreductase catalyzed nitric oxide and reactive oxygen species formation: importance of oxygen concentration. *Nitric Oxide* **2010**, *22*, S24–S24.
- (40) C, M. P. Histochemistry of oxidases in several tissues of bivalve molluscs. *Cell Biol. Int.* **1997**, *21*, 575–584.



- (41) Abele, D.; Heise, K.; Portner, H. O.; Puntarulo, S. Temperature-dependence of mitochondrial function and production of reactive oxygen species in the intertidal mud clam *Mya arenaria*. *J. Exp. Biol.* **2002**, *205*, 1831–1841.
- (42) Suárez-Castillo, E. C.; García-Arrarás, J. E. Molecular evolution of the ependymin protein family: a necessary update. *BMC Evol. Biol.* **2007**, *7*, 23.
- (43) Tang, S. J.; Sun, K. H.; Sun, G. H.; Lin, G.; Lin, W. W.; Chuang, M. J. Cold-induced ependymin expression in zebrafish and carp brain: implications for cold acclimation. *FEBS Lett.* **1999**, *459*, 95–99.
- (44) Smith, R. W.; Cash, P.; Ellefsen, S.; Nilsson, G. E. Proteomic changes in the crucian carp brain during exposure to anoxia. *Proteomics* **2009**, *9*, 2217–2229.
- (45) Shashoua, V. E.; Adams, D. S.; Boyer-Boiteau, A.; Cornell-Bell, A.; Li, F. H.; Fisher, M. Neuroprotective effects of a new synthetic peptide, CMX-9236, in in vitro and in vivo models of cerebral ischemia. *Brain Res.* **2003**, *963*, 214–223.
- (46) Borges, J. C.; Ramos, C. H. Protein folding assisted by chaperones. *Protein Pept. Lett.* **2005**, *12*, 257–261.
- (47) Hamdoun, A. M.; Cheney, D. P.; Cherr, G. N. Phenotypic plasticity of HSP70 and HSP70 gene expression in the Pacific oyster (*Crassostrea gigas*): Implications for thermal limits and induction of thermal tolerance. *Biol. Bull.* **2003**, *205*, 160–169.
- (48) Haslbeck, M.; Franzmann, T.; Weinfurter, D.; Buchner, J. Some like it hot: the structure and function of small heat-shock proteins. *Nat. Struct. Mol. Biol.* **2005**, *12*, 842–846.
- (49) Li, Y.; Qin, J. G.; Abbott, C. A.; Li, X.; Benkendorf, K. Synergistic impacts of heat shock and spawning on the physiology and immune health of *Crassostrea gigas*: an explanation for summer mortality in Pacific oysters. *Am. J. Physiol.: Regul., Integr. Comp. Physiol.* **2007**, *293*, R2353–2362.
- (50) Antoku, K.; Maser, R. S.; Scully, W. J.; Delach, S. M.; Johnson, D. E. Isolation of Bcl-2 binding proteins that exhibit homology with BAG-1 and suppressor of death domains protein. *Biochem. Biophys. Res. Commun.* **2001**, *286*, 1003–1010.
- (51) Szegedi, S. S.; Castro, C. C.; Koutmos, M.; Garrow, T. A. Betaine-homocysteine S-methyltransferase-2 is an S-methylmethionine-homocysteine methyltransferase. *J. Biol. Chem.* **2008**, *283*, 8939–8945.
- (52) Markham, G. D.; Pajares, M. A. Structure-function relationships in methionine adenosyltransferases. *Cell. Mol. Life Sci.* **2009**, *66*, 636–648.
- (53) Wang, C.; Gomer, R. H.; Lazarides, E. Heat shock proteins are methylated in avian and mammalian cells. *Proc. Natl. Acad. Sci. U. S. A.* **1981**, *78*, 3531–3535.
- (54) Cavallaro, R. A.; Fuso, A.; Nicolia, V.; Scarpa, S. S-adenosylmethionine prevents oxidative stress and modulates glutathione metabolism in TgCRND8 mice fed a B-vitamin deficient diet. *J. Alzheimer's Dis.* **2010**, *20*, 997–1002.
- (55) Pernet, F.; Tremblay, R.; Comeau, L.; Guderley, H. Temperature adaptation in two bivalve species from different thermal habitats: energetics and remodelling of membrane lipids. *J. Exp. Biol.* **2007**, *210*, 2999–3014.
- (56) Yao, C. L.; Somero, G. N. Thermal stress and cellular signaling processes in hemocytes of native (*Mytilus californianus*) and invasive (*M. galloprovincialis*) mussels: Cell cycle regulation and DNA repair. *Comp. Biochem. Physiol., Part A* **2013**, *165*, 159–168.
- (57) Perdomo, G.; Dong, H. H. Apolipoprotein D in lipid metabolism and its functional implication in atherosclerosis and aging. *Aging* **2009**, *1*, 17–27.
- (58) Ranganathan, S.; Walsh, E. S.; Godwin, A. K.; Tew, K. D. Cloning and characterization of human colon glyoxalase-I. *J. Biol. Chem.* **1993**, *268*, 5661–5667.
- (59) Fox, I. H.; Kelley, W. N. Phosphoribosylpyrophosphate in Man - Biochemical and Clinical Significance. *Ann. Int. Med.* **1971**, *74*, 424–433.
- (60) Rongvaux, A.; Andris, F.; Van Gool, F.; Leo, O. Reconstructing eukaryotic NAD metabolism. *Bioessays* **2003**, *25*, 683–690.
- (61) Ueda, K.; Hayaishi, O. Adp-Ribosylation. *Annu. Rev. Biochem.* **1985**, *54*, 73–100.
- (62) Crowley, C. L.; Payne, C. M.; Bernstein, H.; Bernstein, C.; Roe, D. The NAD(+) precursors, nicotinic acid and nicotinamide protect cells against apoptosis induced by a multiple stress inducer, deoxycholate. *Cell Death Differ.* **2000**, *7*, 314–326.
- (63) Yu, S. W.; Andrabi, S. A.; Wang, H.; Kim, N. S.; Poirier, G. G.; Dawson, T. M.; Dawson, V. L. Apoptosis-inducing factor mediates poly(ADP-ribose) (PAR) polymer-induced cell death. *Proc. Natl. Acad. Sci. U.S.A.* **2006**, *103*, 18314–18319.
- (64) Hegaret, H.; Wikfors, G. H.; Soudant, P.; Delaporte, M.; Alix, J. H.; Smith, B. C.; Dixon, M. S.; Quere, C.; Le Coz, J. R.; Paillard, C.; Moal, J.; Samain, J. F. Immunological competence of eastern oysters, *Crassostrea virginica*, fed different microalgal diets and challenged with a temperature elevation. *Aquaculture* **2004**, *234*, 541–560.
- (65) Romestand, B.; Corbier, F.; Roch, P. Protease inhibitors and haemagglutinins associated with resistance to the protozoan parasite, *Perkinsus marinus*, in the Pacific oyster, *Crassostrea gigas*. *Parasitology* **2002**, *125*, 323–329.
- (66) Berridge, M. J.; Lipp, P.; Bootman, M. D. The versatility and universality of calcium signalling. *Nat. Rev. Mol. Cell Biol.* **2000**, *1*, 11–21.
- (67) Littarru, G. P.; Tiano, L. Bioenergetic and antioxidant properties of coenzyme Q(10): Recent developments. *Mol. Biotechnol.* **2007**, *37*, 31–37.
- (68) Sevin, D. C.; Sauer, U. Ubiquinone accumulation improves osmotic-stress tolerance in *Escherichia coli*. *Nat. Chem. Biol.* **2014**, *10* (4), 266–272.
- (69) Driessen, H. P. C.; Dejong, W. W.; Tesser, G. I.; Bloemendal, H. The Mechanism of N-Terminal Acetylation of Proteins. *Crit. Rev. Biochem. Mol.* **1985**, *18*, 281–325.
- (70) Desir, G. V. Role of renalase in the regulation of blood pressure and the renal dopamine system. *Curr. Opin. Nephrol. Hypertens.* **2011**, *20*, 31–36.
- (71) Lacoste, A.; Malham, S. K.; Cueff, A.; Jalabert, F.; Gelebart, F.; Poulet, S. A. Evidence for a form of adrenergic response to stress in the mollusc *Crassostrea gigas*. *J. Exp. Biol.* **2001**, *204*, 1247–1255.
- (72) Hoffmann, E. K.; Lambert, I. H.; Pedersen, S. F. Physiology of cell volume regulation in vertebrates. *Physiol. Rev.* **2009**, *89*, 193–277.
- (73) Coquelle, F. M.; Levy, T.; Bergmann, S.; Wolf, S. G.; Bar-El, D.; Sapir, T.; Brody, Y.; Orr, I.; Barkai, N.; Eichele, G.; Reiner, O. Common and divergent roles for members of the mouse DCX superfamily. *Cell Cycle* **2006**, *5*, 976–983.
- (74) Kaplan, A.; Reiner, O. Linking cytoplasmic dynein and transport of Rab8 vesicles to the midbody during cytokinesis by the doublecortin domain-containing 5 protein. *J. Cell Sci.* **2011**, *124*, 3989–4000.
- (75) Montagnani, C.; Tirape, A.; Boulo, V.; Escoubas, J. M. The two Cg-timp mRNAs expressed in oyster hemocytes are generated by two gene families and differentially expressed during ontogenesis. *Dev. Comp. Immunol.* **2005**, *29*, 831–839.
- (76) Raju, R.; Jian, B.; Hooks, J. J.; Nagineni, C. N. Transforming growth factor-beta regulates the expression of anosmin (KAL-1) in human retinal pigment epithelial cells. *Cytokine* **2013**, *61*, 724–727.
- (77) Ko, G. W.; Dineshram, R.; Campanati, C.; Chan, V. B.; Havenhand, J.; Thiyagarajan, V. Interactive effects of ocean acidification, elevated temperature, and reduced salinity on early-life stages of the Pacific Oyster. *Environ. Sci. Technol.* **2014**, *48*, 10079–10088.
- (78) Yamaura, K.; Takahashi, K. G.; Suzuki, T. Identification and tissue expression analysis of C-type lectin and galectin in the Pacific oyster, *Crassostrea gigas*. *Comp. Biochem. Physiol., Part B: Biochem. Mol. Biol.* **2008**, *149*, 168–175.
- (79) Shumway, S. Effect of salinity fluctuation on the osmotic pressure and Na<sup>+</sup>, Ca<sup>2+</sup> and Mg<sup>2+</sup> ion concentrations in the hemolymph of bivalve molluscs. *Mar. Biol.* **1977**, *41*, 153–177.
- (80) Davidson, H. W.; Wenzlau, J. M.; O'Brien, R. M. Zinc transporter 8 (ZnT8) and beta cell function. *Trends Endocrinol. Metab.* **2014**, *25*, 415–424.
- (81) Blaustein, M. P.; Lederer, W. J. Sodium calcium exchange: Its physiological implications. *Physiol. Rev.* **1999**, *79*, 763–854.

(82) Han, Q.; Robinson, H.; Li, J. Y. Biochemical identification and crystal structure of kynurenine formamidase from *Drosophila melanogaster*. *Biochem. J.* **2012**, *446*, 253–260.

(83) Wu, Y. Y.; Peck, K.; Chang, Y. L.; Pan, S. H.; Cheng, Y. F.; Lin, J. C.; Yang, R. B.; Hong, T. M.; Yang, P. C. SCUBE3 is an endogenous TGF-beta receptor ligand and regulates the epithelial-mesenchymal transition in lung cancer. *Oncogene* **2011**, *30*, 3682–3693.

(84) Luna-Acosta, A.; Rosenfeld, E.; Amari, M.; Fruitier-Arnaudin, I.; Bustamante, P.; Thomas-Guyon, H. First evidence of laccase activity in the Pacific oyster *Crassostrea gigas*. *Fish Shellfish Immunol.* **2010**, *28*, 719–726.

(85) Majeran, W.; Zybailov, B.; Ytterberg, A. J.; Dunsmore, J.; Sun, Q.; van Wijk, K. J. Consequences of C4 differentiation for chloroplast membrane proteomes in maize mesophyll and bundle sheath cells. *Mol. Cell. Proteomics.* **2008**, *7*, 1609–1638.